CONFIDENTIAL

Copy
RM E53L17a

NACA RM E53L17a

RESEARCH MEMORANDUM

ROTATING STALL INVESTIGATION OF 0.72 HUB-TIP RATIO SINGLE-STAGE COMPRESSOR

By Robert W. Graham and Vasily D. Prian

Lewis Flight Propulsion Laboratory
Cleveland, Ohio

NATIONAL ADVISORY COMMITTEE
FOR AERONAUTICS

WASHINGTON

March 9, 1954

CONFIDENTIAL

NACA RM E53L17a

NATIONAL ADVISORY COMMITTEE FOR AERONAUTICS

RESEARCH MEMORANDUM

ROTATING STALL INVESTIGATION OF 0.72 HUB-TIP RATIO SINGLE-STAGE COMPRESSOR

By Robert W. Graham and Vasily D. Prian

SUMMARY

The rotating stall characteristics of a 0.72 hub-tip ratio, symmetrical-velocity-diagram design, single-stage compressor were investigated for 60, 70, and 80 percent design speed. The stage was a 14-inch-diameter replica of the fourth stage of an experimental multistage compressor.

Total-span rotating stall patterns with six and eight stall zones were observed at 60 percent and 70 percent design speed. An eight-zone stall pattern was observed at 80 percent design speed before a fatigue failure of some of the rotor blades prevented further investigations of the rotating stall characteristics at other speeds. For the speed range covered in the investigation, the absolute rotation of the stall zone was approximately one-fourth of rotor speed.

When the stall region of the single-stage replica was compared with the part-speed stall operation of the multistage compressor, it was observed that the fourth stage of the multistage operated at appreciably higher flow coefficients than those which corresponded to the rotating stall region of the single-stage replica. Consequently, the fourth stage probably did not incite the stall patterns which were observed during part-speed operation of the multistage compressor.

The failure of the rotor blades was ascribed to blade vibrations promoted by a resonance condition between the rotating stall frequency and the natural bending frequency of the blades. The fundamental of the rotating-stall disturbance frequency coincided with the natural bending frequency of the blades at approximately 75 percent design speed. Metallurgical examination of the fractures indicated that the fatigue fractures had been progressive with an appreciable time interval between the beginning of the first fatigue cycle and the final blade failure.

[redacted]

INTRODUCTION

The purpose of this investigation was to determine the stall characteristics of a 0.72 hub-tip ratio stage which was a scaled-down replica of the fourth stage of the multistage compressor reported in reference 1. This stage was of interest because it was observed that the intensity of the stall disturbance extending throughout the entire length of the multistage compressor diminished appreciably after the fourth stage. Thus, an apparent attenuation of the stall intensity appeared to occur in either the fourth or fifth stages of the compressor. The over-all performance and stall characteristics of a replica of the fifth stage appear in reference 2.

During the course of the investigation in the stall region of operation, a rotor blade failure occurred. Previous experience has demonstrated that the flow fluctuations associated with rotating stall can be sufficiently severe to promote fatigue failures of compressor blading, whenever a resonant condition exists between the stall disturbance frequency and the natural bending frequency of the blades (refs. 3 and 4).

Unfortunately, the stall zone propagation rate and the number of stall zones cannot be predicted currently; consequently, experimental investigations similar to the one described herein are required to obtain these stall data.

SYMBOLS

The following symbols are used in this report:

c_p	specific heat at constant pressure, Btu/(lb)(°F)
D	diffusion factor (see ref. 5)
g	acceleration due to gravity, 32.17 ft/sec^2
h	dimensionless ratio of axial component of air velocity to rotor tip speed
J	mechanical equivalent of heat, 778.3 ft-lb/Btu
P	total pressure, lb/sq ft
T	total temperature, °F
U	wheel speed, ft/sec
V	absolute air velocity, ft/sec

V' relative air velocity, ft/sec

X ratio of circumferential component of absolute velocity of entering air to rotor tip speed

Y ratio of change in circumferential component of velocity to rotor tip speed

Z ratio of blade-element velocity to rotor tip speed

α angle of attack on blade row, deg

β absolute air angle, deg

β' relative air angle, deg

Γ dimensionless blade exciting parameter, $\frac{\text{stall disturbance frequency}}{\text{natural bending frequency}}$

γ ratio of specific heats

η adiabatic efficiency

θ ratio of ambient temperature to NACA standard temperature

λ number of rotating stalls

ν ratio of stall-propagation rate relative to rotor with respect to rotor speed

ρ density of air, lb/cu ft

σ solidity, ratio of chord length to spacing

Φ flow coefficient, V/U_m

Ψ pressure coefficient, isentropic enthalpy rise/$(U_m/\sqrt{\theta})^2$

Subscripts:

ac actual

m evaluated at mean radius

t evaluated at tip radius

z axial component

[redacted]

1 after guide vanes

2 after stator

3 compressor exit (downstream of stators)

Barred symbol indicates average value

APPARATUS AND INSTRUMENTATION

Compressor

The single-stage compressor employed in this investigation consisted of 33 guide vanes, 34 rotor blades, and 35 stator blades. The stage was a 14-inch replica of the fourth stage of the multistage compressor design of reference 6. The hub-tip ratio at the rotor inlet was 0.72. The stage was designed assuming (1) a symmetrical velocity diagram at all radii, (2) approximately constant total enthalpy at all radii, and (3) simplified radial equilibrium to establish the axial velocity distribution. In order to facilitate the manufacture of the blades, the chord length was made constant at all radii. A complete description of the design procedure employed is presented in reference 6. The design data for the stage appear in table I. The diffusion factor presented in table I is a blade loading parameter employed in current design procedure (ref. 5).

In order to duplicate the air exit angles leaving the third-stage stators of the multistage compressor, guide vanes were employed in the single-stage replica to prewhirl the air. The guide vanes were circular-arc, constant-thickness vanes set at zero angle of incidence. They were designed by means of an empirical method described in reference 7 which corrects for secondary flow effects on the guide-vane turning.

Test Facility

The single-stage axial-flow-compressor test facility used in this investigation is the same facility as that described in reference 2.

Instrumentation

The instrumentation is identical to that described in reference 2. Two total-temperature rakes and two 15-tube total-pressure rakes located at the compressor discharge were utilized in measuring the temperature rise and pressure rise across the stage. Radial traverses of these

instruments were made at five radial stations which were area centers of five equal areas in the compressor annulus. Hot-wire anemometer instrumentation similar to that described in reference 8 was employed in detecting the rotating stall patterns and measuring the magnitude of the flow fluctuations associated with rotating stall. The hot-wire probes were located after the stator-blade row.

An audio-frequency oscillator was used in conjunction with the oscilloscope to determine the frequency with which the rotating stall regions passed one of the anemometer probes.

Procedure and Method of Calculation

Over-all performance of the stage was obtained at corrected tip speeds of 498, 568, and 640 feet per second, which correspond, respectively, to 60, 70, and 80 percent design speed. For 60 and 70 percent design speed, the air flow was varied over the entire attainable operating range. At 80 percent design speed, the blade failure prevented a performance investigation over a complete range of weight flows.

The total pressure after the stage was calculated from an arithmetic average of the total-pressure readings obtained from radial surveys at the compressor exit. In order not to penalize the rotor with the total-pressure loss of the inlet guide vanes, the total pressure at the inlet to the rotor was calculated by correcting the depression-tank total pressure for the guide-vane total-pressure loss.

The total-temperature rise across the stage was calculated by arithmetically averaging the total-temperature-rise readings obtained from radial surveys of the flow passage.

While the over-all performance data were being obtained, hot-wire anemometers were employed to detect the stall patterns behind the rotor. Photographic records were made of the rotating-stall patterns viewed on the cathode-ray oscilloscope. The included angle between the hot-wire anemometer probes was varied from 60° to 120° so that sufficient data could be obtained to calculate the number of stall zones present. The number of stall zones was determined by measuring the time interval which elapsed when a given stall zone moved from the first hot-wire probe to the second probe. The method for calculating the number of stalls is described in reference 9. The flow fluctuation parameter $\Delta\rho V/\overline{\rho V}$, which is a measure of the magnitude of the flow disturbance, was calculated according to the procedure described in references 8 and 9.

RESULTS AND DISCUSSION

Over-All Performance

A performance map of the compressor stage described herein is presented in figure 1. The performance is indicated in terms of adiabatic efficiency (ratio of isentropic work to actual work) and dimensionless flow and pressure parameters. The flow coefficient parameter is a ratio of the axial velocity to the wheel velocity at the midspan of the blade. The pressure coefficient is a ratio of the isentropic enthalpy rise to the square of the mean wheel velocity. Providing there are no appreciable changes in the compressibility effects over a range of compressor speeds, the pressure and flow coefficients eliminate rotating speed as a parameter in the presentation of compressor performance data. Although no data were obtained above 80 percent design speed, the performance at the higher speeds would probably not differ from the low-speed performance shown in figure 1, because the Mach number level of compressor operation would not increase sufficiently to change the compressibility effects.

The performance characteristic (pressure coefficient against flow coefficient) did not exhibit any marked discontinuities in the stall region because the stall zones did not develop abruptly across the entire blade span.

Rotating Stall Patterns

In figure 2, the regions of rotating stall observed during the experimental investigation are superposed on the performance map of the compressor. In this figure total-pressure ratio was selected in lieu of the pressure coefficient used in figure 1 so that the stall regions could be illustrated more clearly. The stall zones, in all cases, extended radially over the entire blade span length.

The regions over which specific types of stall pattern prevail are shown shaded on figure 2 and are marked with the number of stall zones. The lightly shaded regions above each curve are the stall patterns observed when the flow coefficient was diminished between each operating point, whereas the darkly shaded regions below each curve are the patterns observed when the flow coefficient was increased. A hysteresis effect was observed in that each stall pattern occurs at higher flow coefficient values when the weight flow is increased rather than decreased. For example, the eight-zone stall pattern at 60 percent of design speed began at a flow coefficient of 0.332 when the flow was decreased, and the stall pattern persisted to a flow coefficient value of 0.396 when the flow was increased.

At 60 and 70 percent design speed, two different stall patterns were observed which contained six and eight stall zones. Data on a stall pattern were being recorded at 80 percent design speed when the blade failure occurred. Several pictures were taken of the stall traces on the oscilloscope screen, but unfortunately the frequency of the stall disturbance was not measured. The film record of the stall traces at 80 percent design speed, shown in figure 3(a), indicates that the traces from both of the hot-wire anemometers were in phase with the angle between the probes set at 90°. A stall pattern with four or eight stall zones would produce this type of film record. Since an eight-zone stall pattern occurred at the lower compressor speeds, it was assumed that the same stall pattern occured at 80 percent design speed. This assumption was justified because the stall pattern at 80 percent design speed began at approximately the same flow coefficient as the eight-zone patterns of the lower speeds. It has been observed that the inception of a given stall pattern is a function of flow coefficient, which is in turn a function of angle of attack.

Previous studies have shown that the stall disturbance frequency of a given number of stall zones varies linearly with compressor speed. A curve of stall disturbance frequency against compressor speed was linearly extrapolated to 80 percent design speed to estimate the disturbance frequency at that speed.

As is observed in figure 2, there was no discontinuous drop in pressure rise across the stage when the periodic stall patterns developed. There was a wide span of flow coefficients just above the region marking the periodic stall patterns where stage stall was apparent, but no periodic stall patterns with established rotational frequencies were observed. The observations of the hot-wire traces in this region indicated that the tip stalled first and that the stall progressed inward toward the hub region. In reference 9, this is referred to as a progressive-type stall.

Table II contains a summary of the stall data and related computed results. Figure 3 shows some of the typical film records of the stall traces for 60, 70, and 80 percent design speed operation.

The compressor stage discussed herein was very similar to the one discussed in reference 2 (fifth stage of the multistage). A comparison of the total-span stall data reveals similarities in the absolute stall disturbance frequencies and the flow coefficients marking the inception of the stall patterns. However, the number of total-span stall zones present was greater for this stage than was reported in reference 2, and consequently the stall frequencies relative to the blades differ for the two cases.

In reference 3, it was shown that rotating stall occurred over most of the useful part-speed operating range of the multistage compressor frequently alluded to in this report. A comparison of the part-speed

stall operation of the multistage with the single-stage replica of the fourth stage revealed that the fourth stage of the multistage operated at an appreciably higher flow coefficient value than that corresponding to the rotating stall region of the single-stage replica. (Data on the individual stage performance of the multistage compressor appear in ref. 1.) Consequently, the fourth stage probably did not incite the stall patterns observed during part-speed operation of the compressor. A similar observation has been made for the fifth stage based on the stall information reported in reference 2. Apparently the diminution of the stall intensity after the fourth stage, already discussed in the INTRODUCTION, can be attributed to the unstalled condition of both the fourth and fifth stages. These stages acted as effective attenuators of the stall disturbance intensity, which nevertheless did persist throughout the entire axial length of the compressor.

Analysis of the Blade Failure

Photographs of the fractured rotor blades are shown in figure 4(a). The blade failure undoubtedly originated with the steel (SAE 4340) rotor blades because they were the only blades which had the characteristic fatigue fractures. Of the 34 rotor blades, 15 showed definite signs of fatigue failure. Figure 4(b) is a close-up view of one of the rotor blades which suffered fatigue over approximately 95 percent of its cross-sectional area. Only a small area at the leading edge and trailing edge of the blade underwent tensile failure. This particular blade exhibited the most pronounced fatigue failure of any of the blades in the rotor and probably initiated the failure of the rotor row.

In reference 4, experimental evidence was presented which indicated that fatigue failures of compressor blades could be attributed to the resonance between the stall harmonics and the natural bending frequency of the blades. In order to determine whether or not rotating stall was the cause of the blade failure reported herein, an analysis was conducted to see if such resonance existed. In figure 5, the frequency of the rotating stall disturbances relative to the rotor reported herein are compared with the dynamic natural bending frequency of the blades. The dynamic natural bending frequency of the blades was calculated by correcting the static natural bending frequency for the centrifugal stiffening effect according to the method described in reference 10. The static natural bending frequency was determined experimentally.

The bending frequencies of the individual blades varied from blade to blade; thus a band is shown in figure 5 rather than a single line. From examination of figure 5, it is evident that a fundamental resonance condition exists between 70 percent and 80 percent of design speed. During the testing program the compressor was operated in this region for appreciable lengths of time. Other resonance conditions may exist with

the stall harmonics at lower speeds, but the magnitudes of the flow fluctuations are not as great as those of fundamental frequency. Then too, the compressor was operated for comparatively short periods of time in the lower speed range (below 60 percent design speed), so these resonance conditions are not considered to have had a very significant effect on the blade failure.

Several compressor blade failures which have occurred at the NACA Lewis laboratory have been attributed to fatigue promoted by rotating stall. References 3, 4, 11, and 12 contain accounts of experiences with blade failures or blade cracking which have occurred in compressors that operated in a stalled condition during a part of their research history. Rotating stall data were not obtained for all the compressors that failed, but each compressor which failed was operated at low flow coefficients that correspond to stalled conditions on the blades. Most of the blade failures attributable to rotating stall have occurred with long blades. However, the failure reported herein reveals that the intensity of stall disturbances is sufficient to fracture shorter and stiffer blades providing a resonance condition occurs between the exciting force and the natural blade frequency. Thus the shorter blades of the rear and middle stages of multistage compressors are subject to fatigue failure whenever they experience a critical stall frequency. Such a stall disturbance may emanate from the inlet stages during part-speed operation and be of sufficient intensity to cause blade failure in the middle or rear stages.

SUMMARY OF RESULTS

The results of the hot-wire anemometer and over-all performance investigation of a 0.72 hub-tip ratio compressor at 60, 70, and 80 percent design speed are summarized as follows:

1. No appreciable discontinuities in the compressor performance characteristic were observed.

2. Rotating stall patterns with six and eight stall zones were observed. The stall zones extended radially over the entire blade passage and rotated at approximately 25 percent rotor speed. The stall patterns were similar to those found in a previous investigation of a 0.76 hub-tip ratio compressor.

3. For decreasing weight flow the flow coefficients which marked the beginning of a definite rotating stall pattern were approximately equal for all compressor speeds. Hysteresis effects shifted the rotating stall regions to higher values of flow coefficient when the weight flow was increased rather than decreased.

4. The compressor reported herein was a replica of the fourth stage of an experimental multistage compressor. The stall data of the replica indicate that the fourth stage of the multistage compressor probably did not instigate any of the part-speed stall patterns observed in tests of the multistage compressor.

5. The blade failure was attributed to fatigue failure in 44 percent of the rotor blades. Blade vibrations occurred whenever the relative rotating stall disturbance frequency was in resonance with the natural bending frequency of the blades. Such blade vibrations probably occurred during operation between 70 percent and 80 percent design speed.

Lewis Flight Propulsion Laboratory
National Advisory Committee for Aeronautics
Cleveland, Ohio, December 4, 1953

REFERENCES

1. Budinger, Ray E., and Serovy, George K.: Investigation of a 10-Stage Subsonic Axial-Flow Research Compressor. IV - Individual Stage Performance Characteristics. NACA RM E53C11, 1953.

2. Graham, Robert W., and Prian, Vasily D.: Experimental and Theoretical Investigation of Rotating-Stall Characteristics of Single-Stage Axial-Flow Compressor with Hub-Tip Ratio of 0.76. NACA RM E53I09, 1953.

3. Huppert, Merle C., Costilow, Eleanor L., and Budinger, Ray E.: Investigation of a 10-Stage Subsonic Axial-Flow Research Compressor. III - Investigation of Rotating Stall, Blade Vibration and Surge at Low and Intermediate Compressor Speeds. NACA RM E53C19, 1953.

4. Huppert, Merle C., Johnson, Donald F., and Costilow, Eleanor L.: Preliminary Investigation of Compressor Blade Vibration Excited by Rotating Stall. NACA RM E52J15, 1952.

5. Lieblein, Seymour, Schwenk, Francis C., and Broderick, Robert L.: Diffusion Factor for Estimating Losses and Limiting Blade Loadings in Axial-Flow-Compressor Blade Elements. NACA RM E53D01, 1953.

6. Johnsen, Irving A.: Investigation of a 10-Stage Subsonic Axial-Flow Research Compressor. I - Aerodynamic Design. NACA RM E52B18, 1952.

7. Lieblein, Seymour: Turning-Angle Design Rules for Constant-Thickness Circular-Arc Inlet Guide Vanes in Axial Annular Flow. NACA TN 2179, 1950.

[redacted]

8. Laurence, James C., and Landes, L. Gene: Auxiliary Equipment and Techniques for Adapting the Constant-Temperature Hot-Wire Anemometer to Specific Problems in Air-Flow Measurements. NACA TN 2843, 1952.

9. Huppert, Merle C.: Preliminary Investigation of Flow Fluctuations During Surge and Blade Row Stall in Axial-Flow Compressors. NACA RM E52E28, 1952.

10. Timoshenko, Stephen: Vibration Problems in Engineering. Second ed., D. Van Nostrand Co., Inc., 1937.

11. Jackson, Robert J.: Analysis of Performance of Four Symmetrical-Diagram-Type Subsonic Inlet-Stage Axial-Flow Compressors. NACA RM E53K03, 1953.

12. Robbins, William H., and Glaser, Frederick W.: Investigation of an Axial-Flow-Compressor Rotor with Circular-Arc Blades Operating up to a Rotor-Inlet Relative Mach Number of 1.22. NACA RM E53D24, 1953.

[redacted]

TABLE I. - DESIGN DATA FOR COMPRESSOR STAGE

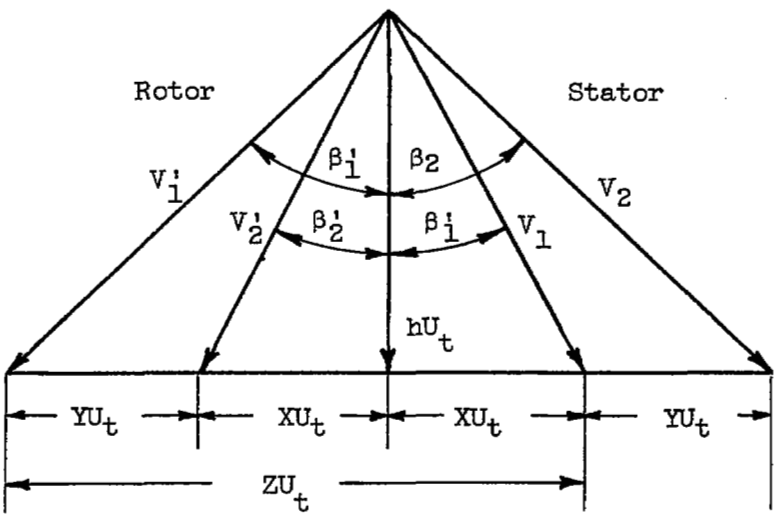

Symmetrical axial-velocity diagram

Z	X	Y	h	V/U_t	β' or β [1]	D	σ	α
Rotor								
0.7197	0.1709	0.3779	0.7591	0.9367	35.87	0.3581	1.067	17.51
.7898	.2227	.3444	.7407	.9328	37.44	.3608	.972	15.59
.8599	.2718	.3163	.7169	.9273	39.36	.3641	.894	14.00
.9300	.3188	.2925	.6873	.9198	41.65	.3688	.826	12.31
1.0000	.3640	.2720	.6517	.9106	44.30	.3747	.768	10.59
Stator								
0.7424	0.1736	0.3808	0.8210	0.9907	34.03	0.3329	1.066	15.46
.8068	.2215	.3504	.7756	.9636	36.41	.3482	.980	14.61
.8712	.2672	.3245	.7257	.9363	39.19	.3650	.908	14.14
.9356	.3110	.3021	.6701	.9082	42.45	.3833	.846	13.76
1.0000	.3533	.2827	.6071	.8793	46.33	.4044	.791	13.65

[1]For rotor, β'; for stator, β.

[redacted]

TABLE II. - SUMMARY OF STALL PATTERNS 0.72 HUB-TIP RATIO

SINGLE-STAGE 14-INCH COMPRESSOR

Compressor speed, percent of design	Lissajous frequency, cps	Number of stalls, λ	Stall-zone frequency, cps	Stall-zone speed / Rotor speed		$\frac{\Delta\rho V}{\overline{\rho V}}$
				Absolute, $1-\nu$	Relative, ν	
60	209	6	34.83	0.258	0.742	0.93
60	278	8	34.75	.258	.742	.73
70	224	6	37.75	.245	.755	1.33
70	302	8	37.75	.245	.755	1.44
80	346	8	43.25	.247	.753	.71

[redacted]

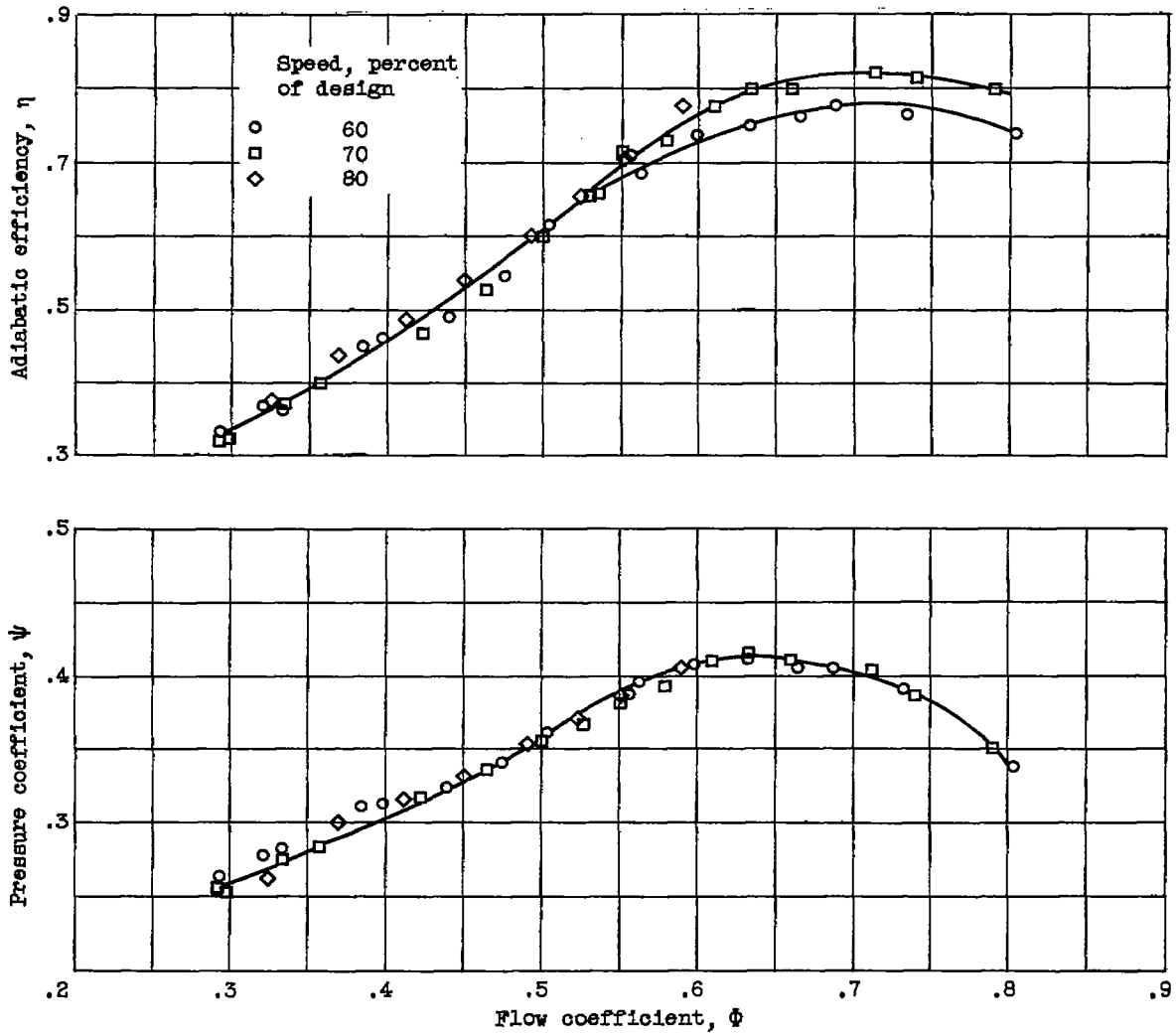

Figure 1. - Performance map of single-stage compressor.

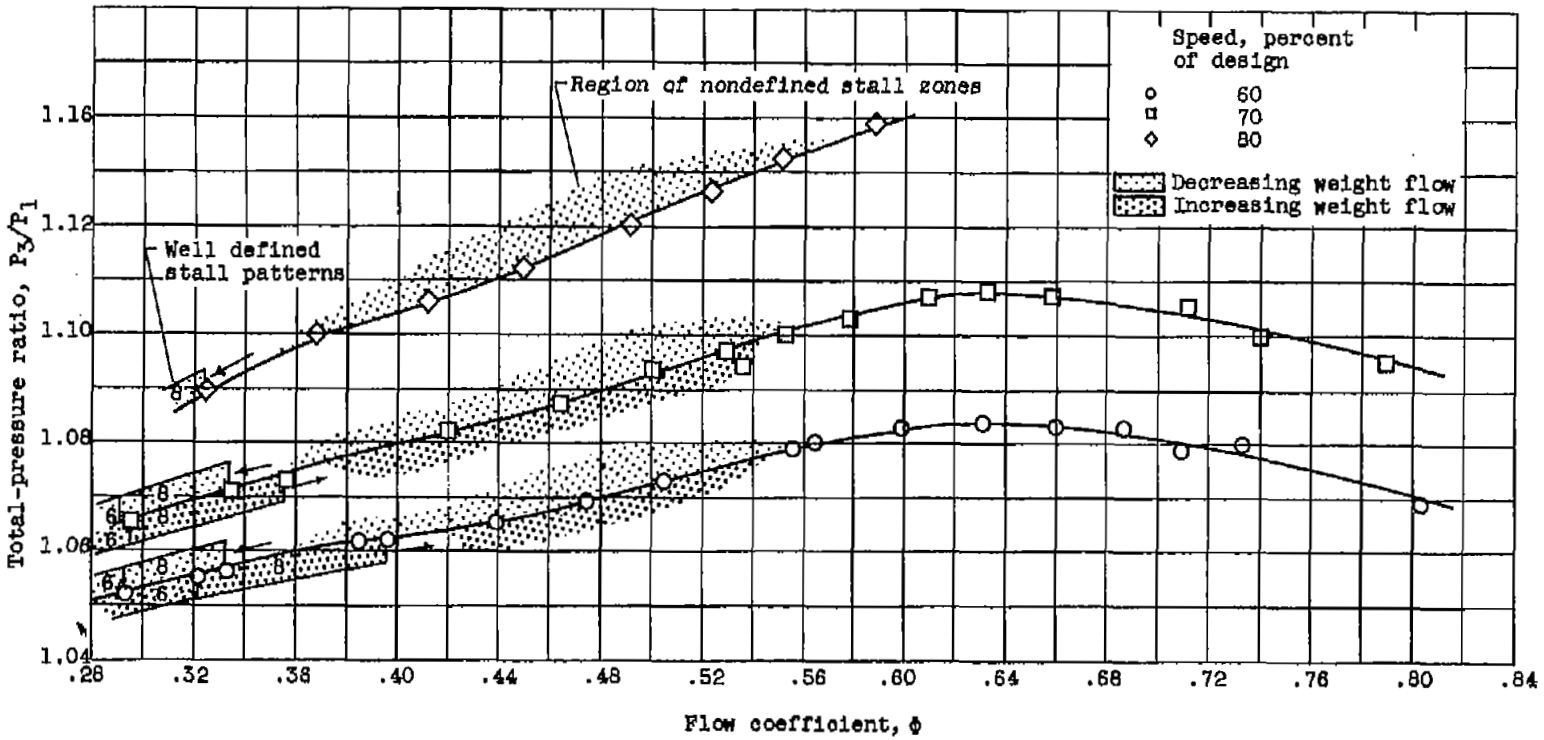

Figure 2. - Rotating stall patterns superposed on performance map of single-stage compressor. (Numbers indicate the number of stall zones.)

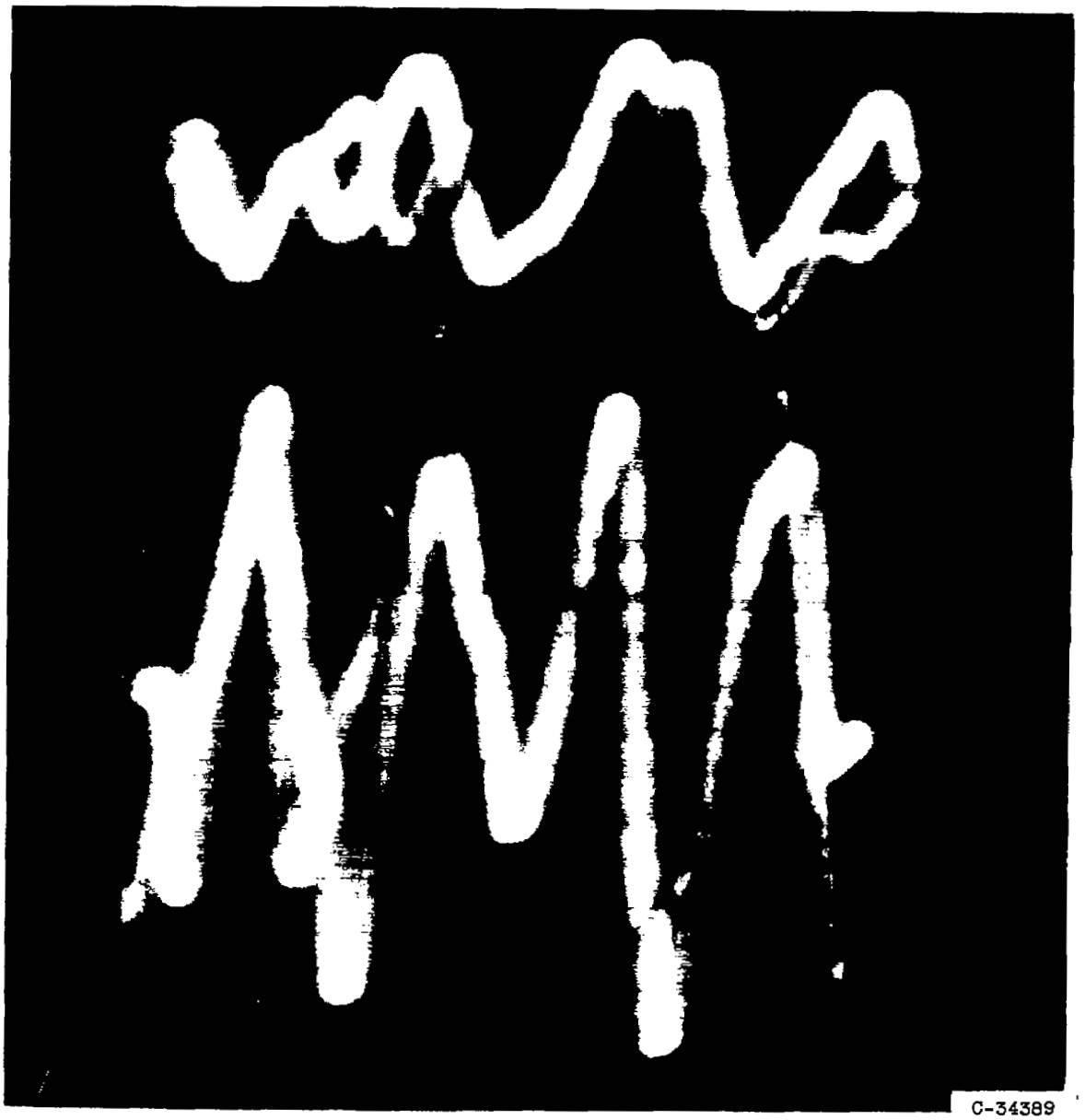

(a) Compressor speed, 80 percent design speed; number of stall zones, 8; frequency, 346 cycles per second; flow coefficient, 0.3244; radial position, A (tip).

Figure 3. - Typical stall patterns observed on cathode-ray oscilloscope.

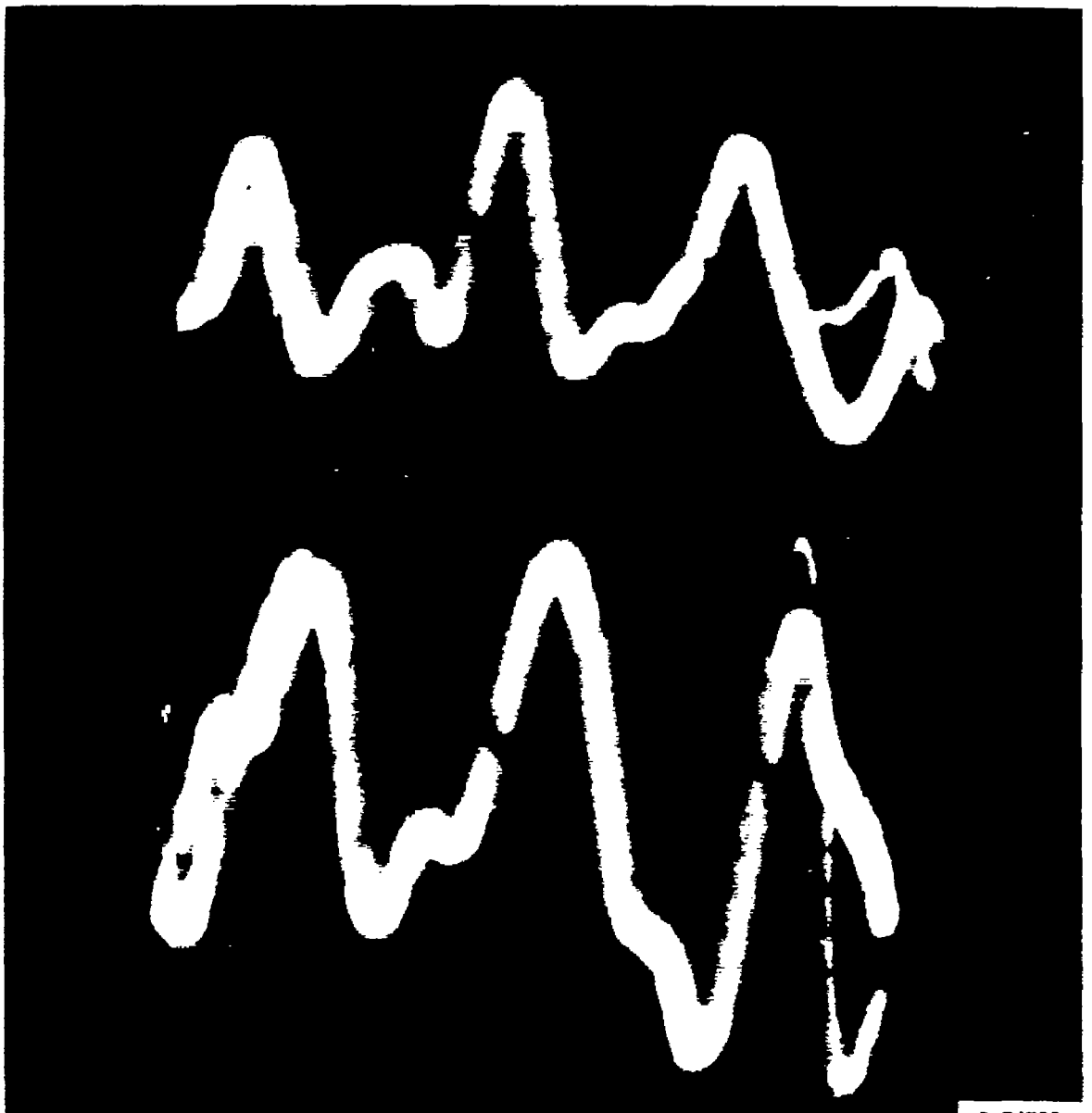

(b) Compressor speed, 70 percent design speed; number of stall zones, 6; frequency, 224 cycles per second; flow coefficient, 0.2746; radial position, B (between tip and midspan).

Figure 3. - Continued. Typical stall patterns observed on cathode-ray oscilloscope.

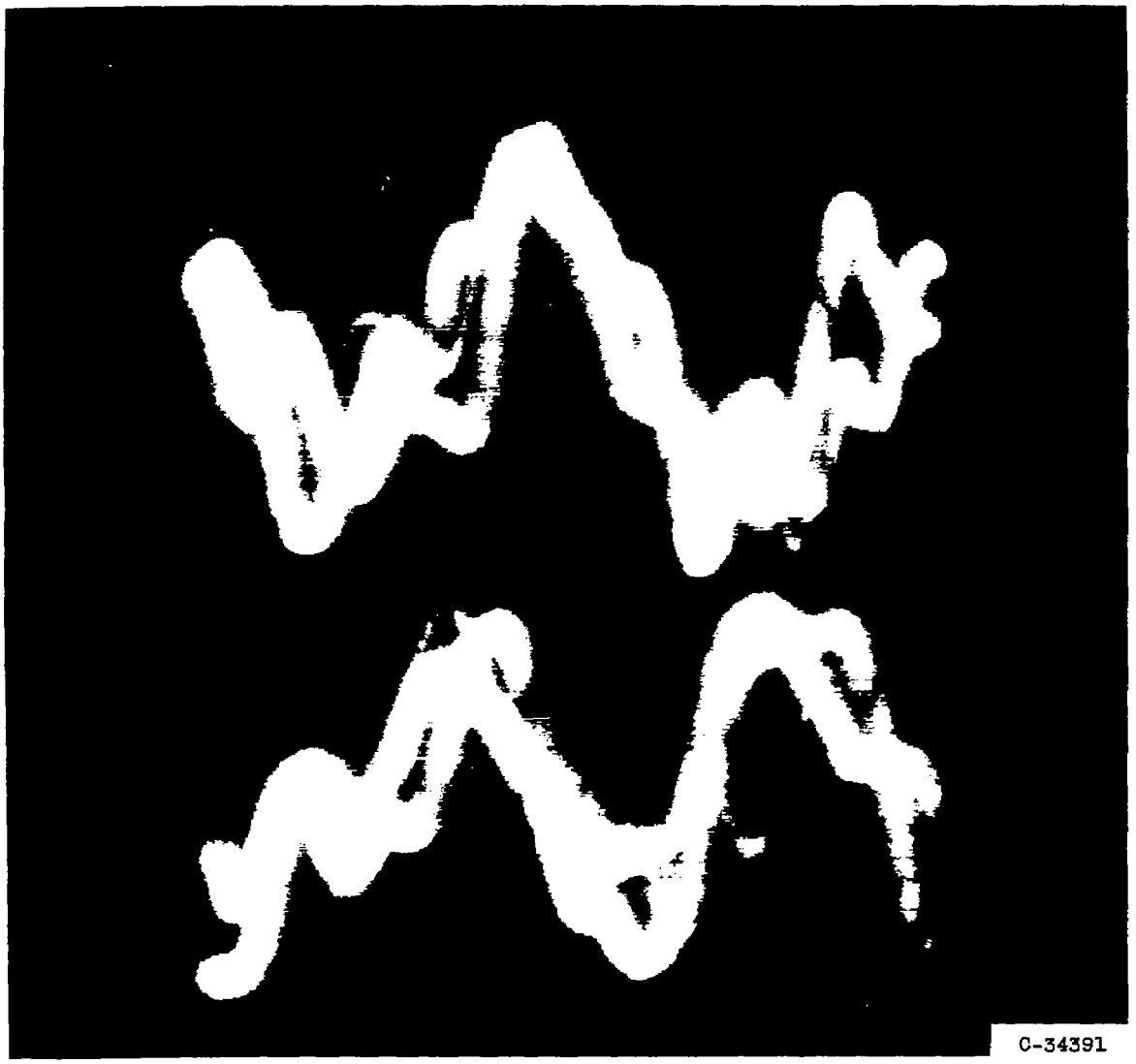

(c) Compressor speed, 60 percent design speed; number of stall zones, 8; frequency, 278 cycles per second; flow coefficient, 0.3328; radial position, A (tip).

Figure 3. - Concluded. Typical stall patterns observed on cathode-ray oscilloscope.

(a) Rotor.

Figure 4. - Blade failures.

(b) Blade having fatigue failure over 95 percent of cross section.

Figure 4. - Concluded. Blade failures.

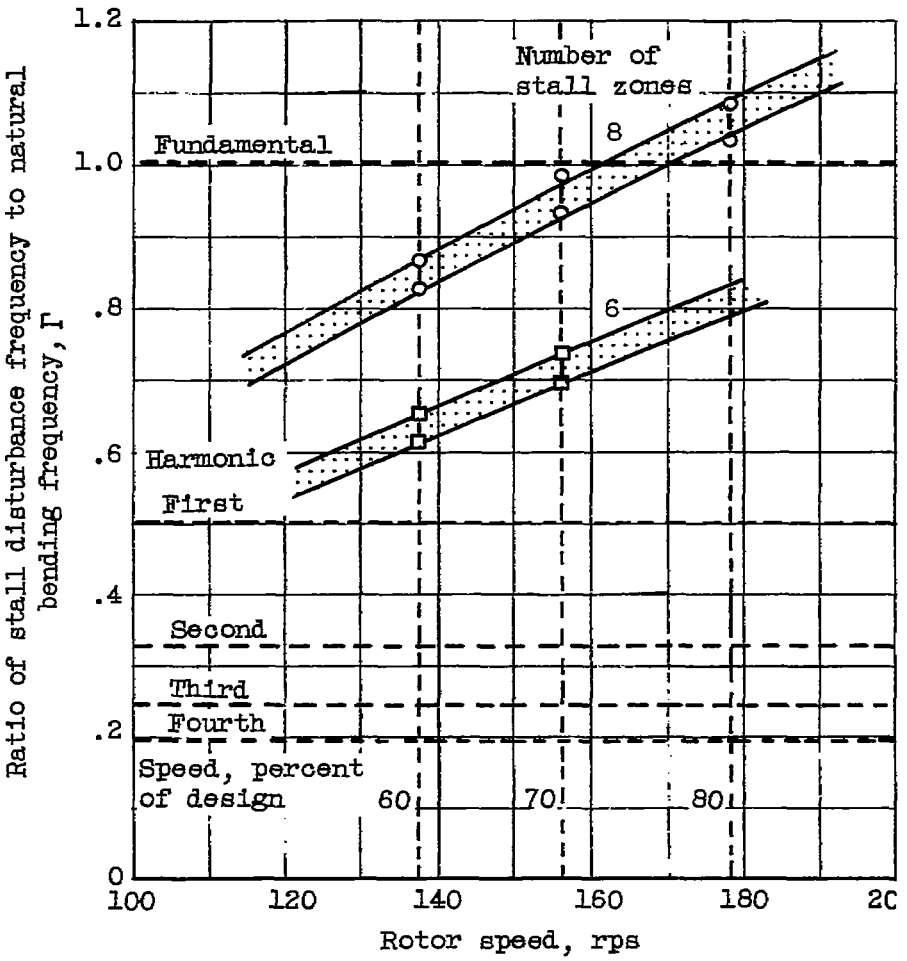

Figure 5. - Dimensionless blade excitation parameter as a function of compressor speed.